TYPE Policy Brief
PUBLISHED 12 September 2022
DOI 10.3389/feart.2022.939964

EDITED BY
Hema Achyuthan,
Anna University, Chennai, India

REVIEWED BY
Yan Li,
China University of Geosciences, China
Xiaomei Nian,
East China Normal University, China

*CORRESPONDENCE
Xue Rui,
xr145@jlu.edu.cn

SPECIALTY SECTION
This article was submitted to Quaternary Science, Geomorphology and Paleoenvironment,
a section of the journal
Frontiers in Earth Science

RECEIVED 09 May 2022
ACCEPTED 15 August 2022
PUBLISHED 12 September 2022

CITATION
Rui X, Li B and Cohen TJ (2022), Testing the use of continental standardized growth curves (SGCs) for D_e estimation on coarse quartz grains from Lake Woods, Northern Australia.
Front. Earth Sci. 10:939964.
doi: 10.3389/feart.2022.939964

Testing the use of continental standardized growth curves (SGCs) for D_e estimation on coarse quartz grains from Lake Woods, Northern Australia

Xue Rui[1,2]*, Bo Li[2,3] and Tim J. Cohen[3,4]

[1]College of Earth Sciences, Jilin University, Changchun, China, [2]Centre for Archaeological Science, School of Earth, Atmospheric and Life Sciences, University of Wollongong, Wollongong, NSW, Australia, [3]ARC Centre of Excellence for Australian Biodiversity and Heritage, University of Wollongong, Wollongong, NSW, Australia, [4]GeoQuest Research Centre, School of Earth, Atmospheric and Life Sciences, University of Wollongong, Wollongong, NSW, Australia

Using continental SGCs built by Fu et al. (2020) can save significant machine time for constructing SGCs when compared to traditional SGC methods, which need significantly more time for building sample-specific or regional SGCs. In this study, the reliability of continental SGCs is tested using coarse quartz grains (180–212 μm) from Lake Woods in Northern Australia. D_e values obtained by continental SGCs are consistent with D_e values obtained by regional SGCs and by the SAR procedures.

KEYWORDS
quartz, lake woods, regional application, luminescence dating, continental standardized growth curves

1 Introduction

Optically stimulated luminescence (OSL) emissions from quartz grains have been widely used for dating sediments in the Quaternary period since the development of the single-aliquot regenerative-dose (SAR) protocol (e.g., Galbraith et al., 1999; Murray and Wintle, 2000; Wintle and Murray, 2006). In the SAR protocol, a dose-response curve (DRC) is constructed for each aliquot using a series of regenerative doses and their corresponding luminescence signals, and the equivalent dose (D_e) is obtained by projecting the natural luminescence signal onto the DRC. However, when there are many samples or the ages of samples are too high, large regenerative doses and long irradiation times are necessary for building a DRC, and the time required for the measurements can be a major impediment of the SAR protocol applications.

To reduce the amount of machine time required, Roberts and Duller (2004) proposed that T_x not only corrects within-aliquot sensitivity changes but can also act as a between-aliquot normalization step. This assumption offers a potential means of creating a standardized growth curve (SGC), from which the D_e can be estimated by projecting the sensitivity-corrected natural OSL signal re-scaled by the corresponding test dose (i.e., L_n/T_n*D_t) onto the SGC, established using a number of re-scaled DRCs obtained from an SAR protocol. This SGC method has been applied to single aliquots of quartz from different regions (e.g., Burbidge et al., 2006; Lai, 2006; Lai et al., 2007; Stevens et al., 2007; Telfer et al., 2008; Long et al., 2010; Yang et al., 2011; Chen et al., 2013; Wang et al., 2022).

To further reduce the inter-aliquot variation of DRCs for quartz OSL from same or different samples, Li et al. (2015) suggested a new method for establishing SGCs by dividing the L_x/T_x data by one of the regenerative dose signals (L_{r1}/T_{r1}). This improved method was called regenerative-dose normalization (re-normalization). By applying this method for a range of quartz samples from different regions of Asia, Africa, Europe, and North America, they constructed a common re-normalized DRC (global standardized growth curve, gSGC) for single aliquots of quartz. With numerical simulation, Peng et al. (2016) showed that the gSGC method is intrinsically more precise than the conventional SGC method.

With the development of the re-normalization method, a similar but improved normalized method was proposed by Li et al. (2016), i.e., the least-squares normalization (LS-normalization). This uses an iterative scaling and fitting procedure that takes all of the L_x/T_x ratios into consideration when constructing the SGC. In addition, Fu et al. (2020) have observed that the DRCs for quartz OSL signals of single grains diverge significantly over ~50 Gy, and a set of continental standardized growth curves (cSGCs) were established for single grains of Australian quartz. With cSGC, a D_e can be determined by measuring the natural signal (L_n), two regenerative-dose signals (L_1 and L_2), and the corresponding test-dose signals (T_n, T_1, and T_2). Significant machine time can be saved for constructing SGCs when compared to traditional SGC methods, which need significantly more time for building sample-specific or regional SGCs (rSGCs). In this study, the reliability of cSGC is tested using coarse quartz grains from Lake Woods in Northern Australia, and the cSGC D_es are compared with the D_e results obtained by the full SAR procedure and also with the results obtained by rSGC.

2 Samples, facilities, and measurement

Lake Woods is an ephemeral freshwater lake in the Northern Territory of Australia (Supplementary Figure S1). One beach sample and four lacustrine samples from three pits of Lake Woods were used to establish rSGC. The deposit type, grain size, and D_e ranges for each sample are summarized in Supplementary Table S1. Each sample was collected from cleaned profile walls using stainless steel tubes. After the tubes were removed, they were immediately wrapped in light-proof plastic and transported to the Luminescence Dating Laboratory at the University of Wollongong for analysis. Quartz grains 180–212 μm in diameter were isolated for OSL dating and purified using the standard procedure (e.g., Wintle, 1997). The measurement was performed on a Risø TL/OSL-DA-20 reader equipped with $^{90}Sr/^{90}Y$ beta sources and green (532 nm) laser for single-grain stimulation. OSL signals were detected by an Electron Tubes 9235B photo-multiplier tube fitted with Hoya U-340 filters.

All single-grain quartz measurements were made using the SAR procedure, and experimental conditions are listed in Supplementary Table S2. The grains were stimulated by a green laser for 1.8 s at 125°C, and the net OSL signal was calculated using the first 0.18 s integral of the initial OSL signal minus a background estimated from the last 0.18 s. The value of the SAR D_e was estimated by interpolating the sensitivity-corrected signals (L_n/T_n) onto the corresponding DRC. Grains were rejected if the resulting OSL data failed to satisfy a series of well-established criteria similar to those proposed by Jacobs et al. (2006), namely, if 1) the initial T_n signal was less than 3σ above its corresponding background or its relative standard error is >25%; 2) the recycling ratio or OSL IR depletion ratio differed from unity by more than 2σ; 3) the recuperation ratio (i.e., the ratio of the L_x/T_x value for the 0 Gy and maximum regenerative dose) is >5%; 4) the figure-of-merit (FOM) value is >10% (Peng and Li, 2017); 5) the reduced chi-square (RCS) value for the DRC is >5 (Peng and Li, 2017); 6) the L_n/T_n ratio is statistically consistent with, or higher than, the saturation level of the corresponding DRC; 7) the D_e value is obtained by extrapolation of the fitted DRC, rather than interpolation among the regenerative-dose signals; and 8) the relative standard error (RSE) of D_e exceeds 50%. It should be noted that full criteria (i.e., all eight criteria) would only be applied for SAR D_e estimation (see below).

3 Results

3.1 Regional SGC determination

A total of 45 aliquots (4,500 grains) from five samples were measured by the SAR procedure, and we rejected grains with poor DRCs based on criteria 1)–5) before building rSGCs (Li et al., 2016; Fu et al., 2020). Within SGC determination, 1) we fitted the measured L_x/T_x data for individual grains using a general-order kinetic (GOK) function, i.e., $(x) = a[1-(1+bcx)^{(-\frac{1}{c})}]+d$, where x represents the radiation dose and a, b, c, and d are constants (Guralnik et al., 2015; Li et al., 2016). We chose this function here because it has proved to be flexible and robust for fitting DRCs with different shapes (see Peng and Li, 2017),and then, the ‘signal growth ratio’ (SGR), defined as the ratio between the L_x/T_x values at 200 and 50 Gy based on the best-fit DRCs for individual grains, is calculated. 2) The SGRs of all investigated grains were divided into k groups using the finite mixture model (FMM) (Roberts et al., 2000), with a zero overdispersion value

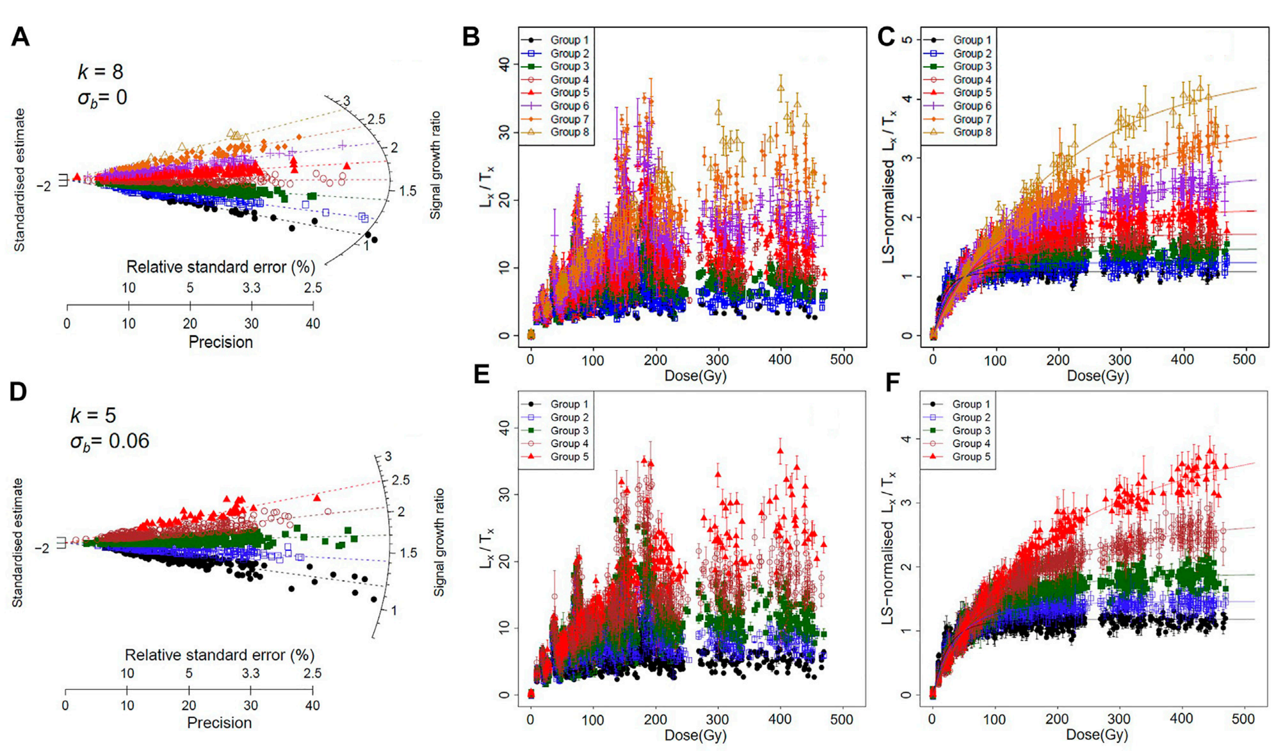

FIGURE 1
(A) Distribution of signal growth ratios for all accepted quartz grains (n = 1,438) from five Lake Woods samples. Different symbols denote the eight groups identified using the finite mixture model and a σ_b value of 0 for each group. **(B)** Single-grain L_x/T_x ratios for the eight groups, plotted as a function of laboratory dose. **(C)** LS-normalized L_x/T_x ratios for the eight groups, based on the data shown in **(B)**. **(D)** Same data in **(A)** but divided into five groups by the FMM (σ_b = 0.06). **(E)** Single-grain L_x/T_x ratios for the five groups in **(D)**. **(F)** LS-normalized L_x/T_x ratios for the five groups, based on the data shown in **(E)**.

(σ_b = 0) for each group (i.e., assuming that the sources of error associated with the signal intensity have been adequately taken into account, see details in Hu et al., 2019). To determine the optimal number of rSGC groups, k was increased from 2 to 10. The optimal number of groups was then estimated as the one associated with the lowest Bayesian information criterion (BIC). 3) The LS-normalization procedure was applied separately to each group to determine their group-specific SGCs.

The SGRs for all the investigated grains are shown in Figure 1A. A large range of SGRs from ~1 to ~3 was observed, indicating that grains have a wide range of saturation doses. For example, the grains with SGRs close to 1.08 (marked by black circle in Figure 1A) correspond to early saturated grains (i.e., there was a negligible increase in the OSL signal beyond 50 Gy). In contrast, grains with L_x/T_x ratios close to 2.85 (marked by yellow triangle in Figure 1A) have a large saturation dose level (keep growing even after 400 Gy). Figure 1C displays the LS-normalized L_x/T_x ratios and common SGCs for all eight groups as a function of the dose. To test the validity of the groupings and establishment of the SGCs, we calculated the ratio between the individual LS-normalized L_x/T_x values and their expected values (based on the best-fit curve) for all the regenerative doses greater than zero. The ratios are plotted in radial plots in Supplementary Figure S2. Around 89–95% of the measured-to-SGC ratios for each group are consistent with unity at 2σ. We propose, therefore, that the DRCs of the Lake Woods quartz grains mentioned here can be represented by eight common SGCs; the best-fit GOK parameters for each SGC are summarized in Supplementary Table S3. Comparing with cSGC (k =6, Supplementary Table S3), our rSGCs have more group numbers and thus have different GOK parameters. When building cSGCs, Fu et al., (2020) assumed all groups have the same σ_b value (0.06). As a 6% overdispersion accounts for the between-grain differences in the DRCs, it may lead to a smaller group number for cSGCs. For a better comparison with the cSGCs, we repeated the building of the rSGC steps but with a fixed σ_b value (σ_b = 0.06), and the calculated optimal k is 5 (Figures 1D–F). As samples for rSGCs were from the same region (i.e., Lake Woods), the fewer groups (with σ_b value of 0.06) than cSGC may contribute to relatively similar OSL properties (e.g., inherent brightness or the shape of the OSL decay curve) of the individual quartz grains. About 90–93% of the measured-to-SGC ratios for each group from five group SGCs (σ_b = 0.06) are consistent with unity at 2σ

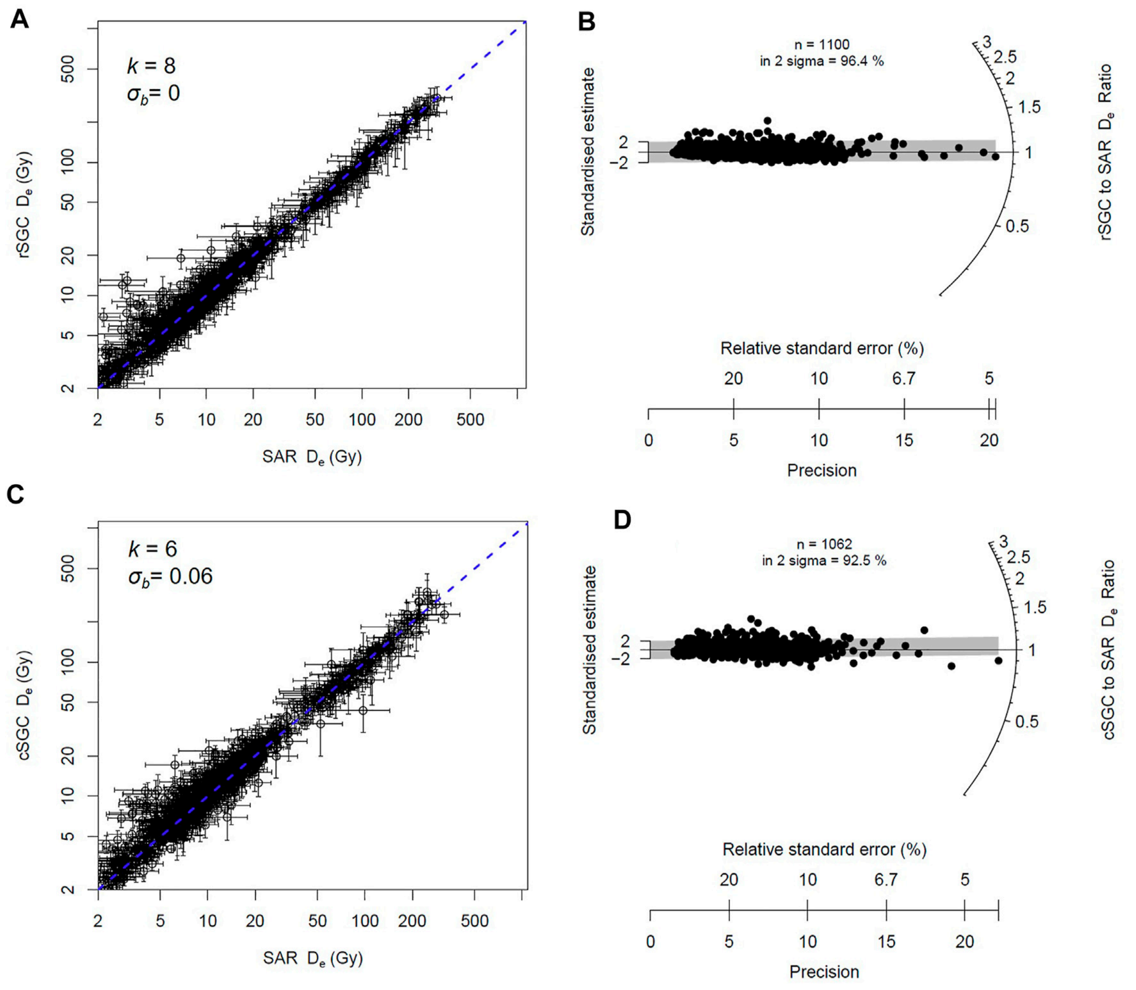

FIGURE 2
(A) Comparison of the SAR and rSGC D_e values (σ_b = 0). The dashed line represents the 1:1 ratio. The ratios of the rSGC and SAR D_e are radially plotted in **(B)**. **(C)** Comparison of the SAR and cSGC D_e values, and the corresponding ratios are radially plotted in **(D)**.

(Supplementary Figure S3). The validation of these two sets of rSGCs is tested in Section 3.2.

3.2 Regional SGC verification

To validate D_e estimates generated by rSGCs, a practical test must demonstrate that the rSGC method can adequately generate the same results as a full SAR protocol. During building of the rSGCs, each grain was assigned to one of the eight groups ($\sigma_b = 0$) or to one of the five groups (σ_b = 0.06) (step 2), and the natural signal has been normalized when applying the LS-normalization procedure to each group to determine their group-specific SGCs (step 3). Thus, the normalized natural signal can directly project onto the corresponding SGC to estimate the D_e value for that grain. The obtained SGC D_e values for all non-rejected grains are compared to the SAR D_e values obtained from individual DRCs (Figure 2A and Supplementary Figure S4A). For the SGCs, D_e values were obtained by eight group SGCs (σ_b = 0), and the two sets of D_e values are in good agreement, with 96.4% of the ratios (rSGC D_e/SAR D_e) consistent with unity at 2σ (Figure 2B). Similarly, the ratios are with 94.4% consistency with unity at 2σ for rSGC D_e values obtained by five group SGCs (σ_b = 0.06) (Supplementary Figure S4B).

It should be noted that the comparisons between the SAR and rSGC D_e values shown in Figure 2A and Supplementary Figure S4A are only available for those grains that produce reliable results using both approaches. As shapes for DRCs and for rSGCs are different, the number of grains that pass criteria 6)–8) is also different (Supplementary Table S4). To further test the reliability of the rSGCs, we compared the D_e distributions of three representative Lake Woods samples

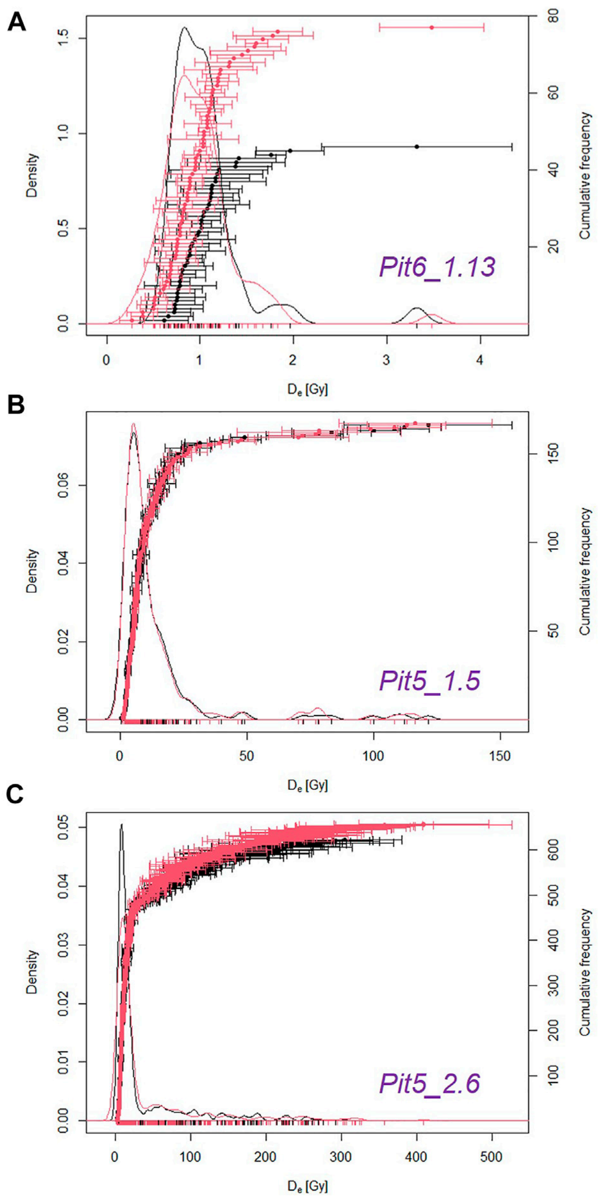

FIGURE 3
Comparison of the D_e values derived using SAR DRCs (black color) and those derived using rSGCs (σ_b =0, red color). **(A)** Sample Pit 6_1.13; **(B)** Sample Pit5_1.15; **(C)** Sample Pit5_2.6.

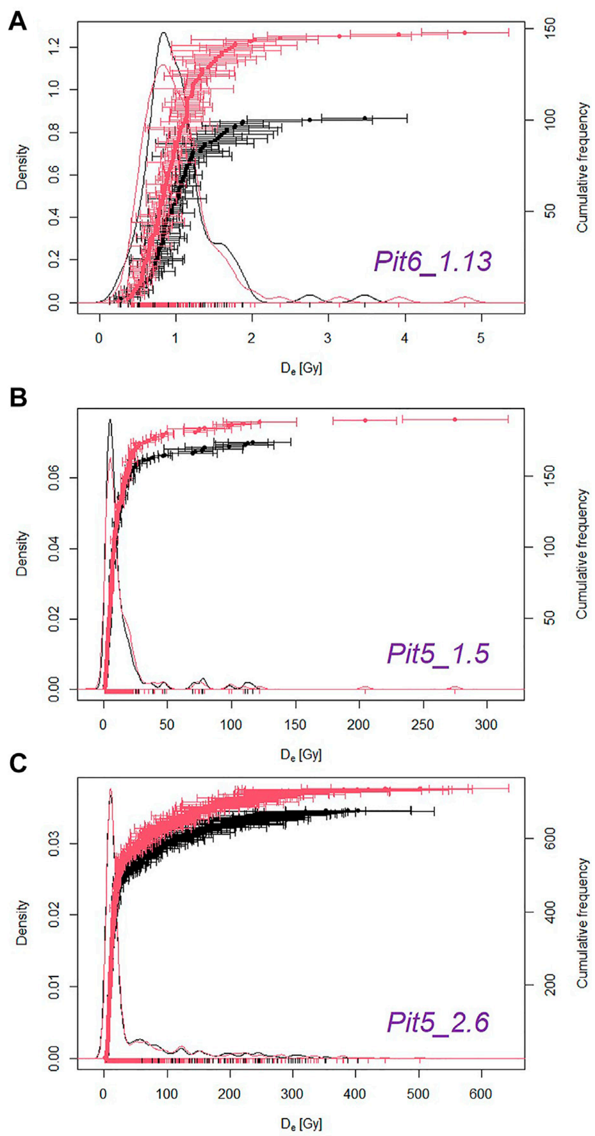

FIGURE 4
Comparison of the D_e values derived using rSGCs (σ_b =0, black color) and those derived using cSGCs (red color). **(A)** Sample Pit 6_1.13; **(B)** Sample Pit5_1.15; **(C)** Sample Pit5_2.6.

(Pit5_1.5, Pit5_2.6, and Pit6_1.13) in Figure 3 and Supplementary Figure S5. For a well-bleached beach sample (Pit6_1.13), the SAR and rSGC D_e (σ_b = 0) distributions have overdispersion values of 20.0 ± 4.8 and 29.8 ± 2.9%, respectively, with most individual D_e values spread randomly about a weighted mean D_e of ~0.98 Gy (Figure 3A). As the CAM D_es are consistent at 2σ (Table 1), we suggest that this increased spread for rSGC D_es does not affect the weighted mean D_e to a significant extent, and similar observations were previously stated by Fu et al. (2020). For lacustrine samples (Pit5_1.5 and Pit5_2.6), both of them showed broad and continuous distribution of D_e values (Figures 3B,C); the corresponding OD values are 94.9 and 106.0% for SAR D_es and 93.3 and 113.1% for rSGC D_es (σ_b = 0). The large spread in D_e may be due to heterogeneous bleaching prior to deposition and/or reworking by bioturbation. In addition to CAM D_e, the Minimum Age Model (MAM) was also applied to these samples to partly identify well-bleached grains. Except the CAM D_e value for Pit5_2.6, the weighted mean D_e values by different

TABLE 1 Weighted mean D_e values for SAR, rSGC, and cSGC. A σ_b value of 0.3 was applied for MAM D_e estimation.

Sample	No. of grains	OD	Approach	Age model 1	D_e (Gy)	Age model 2	D_e (Gy)
Pit6_1.13	53	20.0 ± 4.8	SAR	CAM	0.98 ± 0.04		
	101	29.8 ± 2.9	rSGC (σ_b = 0)	CAM	0.95 ± 0.03		
	101	29.3 ± 2.8	rSGC (σ_b = 0.06)	CAM	0.96 ± 0.03		
	148	36.2 ± 2.6	cSGC	CAM	0.93 ± 0.03		
Pit5_1.5	168	94.9 ± 5.4	SAR	CAM	7.68 ± 0.57	MAM	2.31 ± 0.25
	174	93.3 ± 5.1	rSGC (σ_b = 0)	CAM	7.87 ± 0.56	MAM	2.30 ± 0.22
	176	100.1 ± 5.5	rSGC (σ_b = 0.06)	CAM	8.18 ± 0.63	MAM	2.21 ± 0.22
	190	101.0 ± 5.3	cSGC	CAM	8.40 ± 0.62	MAM	2.14 ± 0.21
Pi5_2.6	626	106.0 ± 3.1	SAR	CAM	17.19 ± 0.74	MAM	7.92 ± 0.30
	678	113.1 ± 3.1	rSGC (σ_b = 0)	CAM	19.00 ± 0.84	MAM	7.67 ± 0.30
	685	114.1 ± 3.2	rSGC (σ_b = 0.06)	CAM	19.53 ± 0.86	MAM	7.75 ± 0.30
	738	113.5 ± 3.0	cSGC	CAM	19.50 ± 0.82	MAM	7.57 ± 0.36

measurement methods (i.e., SAR and rSGC) for these samples are consistent at 2σ (Table 1). Sample Pit5_2.6 includes grains with large D_e values, and around 124 grains (account for 20% of accepted grains) were rejected for criteria 6) and 7) (Supplementary Table S4), which lead to truncation of the full D_e distribution. As the shape for DRCs is different from that of rSGCs, few grains (i.e., 66 grains, account for 10% of accepted grains) were rejected because of extrapolation or saturation. With reduced impact by truncation, the obtained CAM D_e increased from 17.2 ± 0.7 Gy (by SAR data) to 19.0 ± 0.8 Gy (by rSGC data) (Table 1). Regardless of the saturated grains, the general consistency between SAR and rSGC D_es (σ_b = 0) supports that rSGCs perform well for Lake Woods samples. In addition, the OD and the D_e estimates by the CAM and MAM obtained by eight group SGCs are in agreement with those for D_es obtained by five group SGCs (Table 1), and we suggest both rSGC sets are reliable for D_e estimation in Lake Woods.

3.3 Continental SGC verification

In an ideal situation (i.e., the cSGC is reliable for samples from Lake Woods), only three SAR cycles are necessary for cSGC D_e estimation, which involves one cycle for the natural signal and two for regenerative doses, and rejection criteria 1), 4), 6), 7), and 8) can be applied to them. Thus, for each grain, we selected the natural signal, the signal for the second lowest regenerative dose (the lowest being 0 Gy), which lies in the linear portion of the DRC, and the signal for the largest or second largest regenerative dose (which lies beyond the linear region) for cSGC D_e calculation. Using this approach, more grains are accepted than that for SAR or rSGC analysis (Supplementary Table S4). The two selected regenerative doses were referred as D_{r1} and D_{r2}, respectively. The ratio between the L_x/T_x values of D_{r1} and D_{r2} for each accepted grain is calculated, and the obtained ratio is compared with the corresponding ratio for each of the six cSGCs; the latter ratios were calculated by dividing the SGC values at D_{r2} by those at D_{r1}. As the L_x/T_x ratio can quantify the saturation characteristics (e.g., shape of DRC or SGC) of different grains or different group SGCs (Li et al., 2016), this comparison can help us select the specific SGC with similar saturation characteristics to the studied grain. Based on this step, each grain was assigned to one of the six groups from Fu et al., (2020). To normalize the natural signal, the L_{r1}/T_{r1} and L_{r2}/T_{r2} for each grain are multiplied by a scaling factor, such that the sum of squared residuals is minimized. With the scaling factor, the normalized L_n/T_n value can be projected onto the relevant cSGCs to get cSGC D_e, and the obtained cSGC D_e show excellent statistical consistency with the SAR D_e (Figure 2C) and with the rSGC D_e estimates (Supplementary Figure S6A). Around 92.5% of the cSGC-to-SAR D_e ratios (Figure 2D) and 93.9% of the cSGC-to-rSGC D_e ratios (Supplementary Figure S6B) are within 2σ, which validate the use of cSGCs for rapid and robust D_e estimation for quartz grains from Lake Woods.

D_e distributions for the three representative samples (discussed in Section 3.2) are visualized using probability density plots in Figure 4, and the patterns of D_e distributions are generally consistent between the cSGC and rSGC datasets. The OD and the D_e estimates by the CAM and MAM for D_es obtained by cSGC are in agreement with those for D_es obtained by rSGC (Table 1), which further prove the reliability of cSGCs.

4 Conclusion

The application of the cSGC (following Fu et al., 2020) has been successfully verified for coarse-grained quartz samples from Lake Woods. For samples without saturated grains, the D_e values obtained by the cSGC are consistent with the D_e values obtained by the rSGCs and by the SAR procedures. With the verification of the cSGCs, at least 50% of instrument time can be saved comparing the traditional SAR procedure (three SAR cycles for cSGC D_e vs. around seven cycles for SAR D_e measurement), and large instrument time for building rSGC can also be saved (~440 h in this study).

Author contributions

TC conducted the field investigation and collected all samples. XR and TC carried out all the laboratory work. XR, BL, and TC conducted the data analysis and manuscript writing.

Funding

This study was supported by an Australian Research Council (ARC) Future Fellowship to Bo Li (FT140100384), a Foundation for Outstanding Young Teachers in Jilin University to Xue Rui (Grant No. 419080520486), and the ARC Centres of Excellence scheme (Project Number CE170100015) and the ARC Future Fellowship scheme (FT180100524) to Tim Cohen.

Acknowledgments

We thank Richard G. Roberts, Zenobia Jacobs, Yasaman Jafar, and Terry Lachlan for essential support in the luminescence dating laboratory. The open-access publication fee will be provided by Jilin University.

Conflict of interest

The authors declare that the research was conducted in the absence of any commercial or financial relationships that could be construed as a potential conflict of interest.

Publisher's note

All claims expressed in this article are solely those of the authors and do not necessarily represent those of their affiliated organizations, or those of the publisher, the editors, and the reviewers. Any product that may be evaluated in this article, or claim that may be made by its manufacturer, is not guaranteed or endorsed by the publisher.

Supplementary material

The Supplementary Material for this article can be found online at: https://www.frontiersin.org/articles/10.3389/feart.2022.939964/full#supplementary-material

References

Burbidge, C., Duller, G., and Roberts, H. (2006). D_e determination for young samples using the standardised OSL response of coarse-grain quartz. *Radiat. Meas.* 41, 278–288. doi:10.1016/j.radmeas.2005.06.038

Chen, G. Q., Yi, L., Xu, X. Y., Yu, H. J., Cao, J. R., Su, Q., et al. (2013). Testing the standardized growth curve (SGC) to OSL dating coastal sediments from the south Bohai Sea, China. *Geochronometria* 40, 101–112. doi:10.2478/s13386-013-0103-z

Fu, X., Li, B., Jacobs, Z., Jankowski, N. R., Cohen, T. J., and Roberts, R. G. (2020). Establishing standardised growth curves (SGCs) for OSL signals from individual grains of quartz: A continental-scale case study. *Quat. Geochronol.* 60, 101107. doi:10.1016/j.quageo.2020.101107

Galbraith, R. F., Roberts, R. G., Laslett, G. M., Yoshida, H., and Olley, J. M. (1999). Optical dating of single and multiple grains of quartz from jinmium rock shelter, northern Australia: Part I, experimental design and statistical models. *Archaeometry* 41, 339–364. doi:10.1111/j.1475-4754.1999.tb00987.x

Guralnik, B., Li, B., Jain, M., Chen, R., Paris, R. B., Murray, A. S., et al. (2015). Radiation-induced growth and isothermal decay of infrared-stimulated luminescence from feldspar. *Radiat. Meas.* 81, 224–231. doi:10.1016/j.radmeas.2015.02.011

Hu, Y., Li, B., and Jacob, Z. (2019). Single-grain quartz OSL characteristics: Testing for correlations within and between sites in Asia, Europe and Africa. *Methods Protoc.* 3 (1), 2. doi:10.3390/mps3010002

Jacobs, Z., Duller, G. A. T., and Wintle, A. G. (2006). Interpretation of single grain distributions and calculation of. *Radiat. Meas.* 41, 264–277. doi:10.1016/j.radmeas.2005.07.027

Lai, Z.-P., Brückner, H., Zöller, L., and Fülling, A. (2007). Existence of a common growth curve for silt-sized quartz OSL of loess from different continents. *Radiat. Meas.* 42, 1432–1440. doi:10.1016/j.radmeas.2007.08.006

Lai, Z. (2006). Testing the use of an OSL standardised growth curve (SGC) for determination on quartz from the Chinese Loess Plateau. *Radiat. Meas.* 41, 9–16. doi:10.1016/j.radmeas.2005.06.031

Li, B., Jacobs, Z., and Roberts, R. G. (2016). Investigation of the applicability of standardised growth curves for OSL dating of quartz from Haua Fteah cave, Libya. *Quat. Geochronol.* 35, 1–15. doi:10.1016/j.quageo.2016.05.001

Li, B., Roberts, R. G., Jacobs, Z., and Li, S.-H. (2015). Potential of establishing a 'global standardised growth curve' (gSGC) for optical dating of quartz from sediments. *Quat. Geochronol.* 27, 94–104. doi:10.1016/j.quageo.2015.02.011

Long, H., Lai, Z., Fan, Q., Sun, Y., and Liu, X. (2010). Applicability of a quartz OSL standardised growth curve for De determination up to 400 Gy for lacustrine sediments from the Qaidam Basin of the Qinghai-Tibetan Plateau. *Quat. Geochronol.* 5, 212–217. doi:10.1016/j.quageo.2009.05.005

Murray, A. S., and Wintle, A. G. (2000). Luminescence dating of quartz using an improved single-aliquot regenerative-dose protocol. *Radiat. Meas.* 32, 57–73. doi:10.1016/s1350-4487(99)00253-x

Peng, J., and Li, B. (2017). Single-aliquot regenerative-dose (SAR) and standardised growth curve (SGC) equivalent dose determination in a batch model using the R package 'numOSL. *Anc. TL* 35, 32–53. http://ancienttl.org/ATL_35-2_2017/ATL_35-2_Peng_p32-53.pdf.

Peng, J., Pagonis, V., and Li, B. (2016). On the intrinsic accuracy and precision of the standardised growth curve (SGC) and global-SGC (gSGC) methods for equivalent dose determination: A simulation study. *Radiat. Meas.* 94, 53–64. doi:10.1016/j.radmeas.2016.09.006

Roberts, H., and Duller, G. A. (2004). Standardised growth curves for optical dating of sediment using multiple-grain aliquots. *Radiat. Meas.* 38, 241–252. doi:10.1016/j.radmeas.2003.10.001

Roberts, R. G., Galbraith, R., Yoshida, H., Laslett, G., and Olley, J. M. (2000). Distinguishing dose populations in sediment mixtures: A test of single-grain optical dating procedures using mixtures of laboratory-dosed quartz. *Radiat. Meas.* 32, 459–465. doi:10.1016/s1350-4487(00)00104-9

Stevens, T., Armitage, S. J., Lu, H., and Thomas, D. S. (2007). Examining the potential of high sampling resolution OSL dating of Chinese loess. *Quat. Geochronol.* 2, 15–22. doi:10.1016/j.quageo.2006.03.004

Telfer, M., Bateman, M., Carr, A., and Chase, B. (2008). Testing the applicability of a standardized growth curve (SGC) for quartz OSL dating: Kalahari dunes, South African coastal dunes and Florida dune cordons. *Quat. Geochronol.* 3, 137–142. doi:10.1016/j.quageo.2007.08.001

Wang, X., Qiu, F., Nian, X., Liu, R., and Zhang, W. (2022). Testing the applicability of standardised growth curves (SGCs) for OSL signals of quartz grains from the Yangtze Delta, China. *Quat. Geochronol.* 72, 101348. doi:10.1016/j.quageo.2022.101348

Wintle, A. G. (1997). Luminescence dating: Laboratory procedures and protocols. *Radiat. Meas.* 27, 769–817. doi:10.1016/s1350-4487(97)00220-5

Wintle, A. G., and Murray, A. S. (2006). A review of quartz optically stimulated luminescence characteristics and their relevance in single-aliquot regeneration dating protocols. *Radiat. Meas.* 41, 369–391. doi:10.1016/j.radmeas.2005.11.001

Yang, L., Lai, Z., Long, H., and Zhang, J. (2011). Construction of a quartz OSL standardised growth curve (SGC) for aeolian samples from the Horqin dunefield in northeastern China. *Geochronometria* 38, 391–396. doi:10.2478/s13386-011-0045-2